Case Studies in Construction Materials 15 (2021) e00709

Contents lists available at ScienceDirect

Case Studies in Construction Materials

journal homepage: www.elsevier.com/locate/cscm

Case study

The effects of cement type and expanded vermiculite powder on the thermo- mechanical characteristics and durability of lightweight mortars at high temperature and RSM modelling

Fuat Koksal [a], Turan Nazlı [a], Ahmet Benli [b,*], Osman Gencel [c], Gokhan Kaplan [d]

[a] *Department of Civil Engineering, Yozgat Bozok University, 66900 Yozgat, Turkey*
[b] *Department of Civil Engineering, Bingol University, 12100 Bingol, Turkey*
[c] *Department of Civil Engineering, Bartin University, 74100 Bartin, Turkey*
[d] *Department of Civil Engineering, Ataturk University, 25030 Erzurum, Turkey*

ARTICLE INFO

Keywords:
Mortar
High temperature
Expanded vermiculite
Calcium aluminate cement
Thermal and mechanical properties
Durability

ABSTRACT

The results of the impact of cement type and expanded vermiculite powder (EVP) on the thermal, mechanical characteristics and durability of lightweight mortars at high temperature and RSM modelling are presented in the paper. The lightweight mortars were fabricated by replacing fine aggregate with EVP in certain proportions. In the production of the mixtures, two different cement types namely, Portland cement (PC) and calcium aluminate cement (CAC) were used as binders and fine aggregates were replaced with EVP at the rates of 0%, 15%, 30% and 45%. The microstructure, thermal, mechanical properties and durability of PC and CAC mortars produced in this way were determined after standard curing for 28 days at temperatures ranging from 20 °C to 900 °C. Mechanical performance of mortar mixtures was evaluated based on compressive, flexural strength and ultrasonic pulse velocity (UPV). The durability of the specimens was also determined using porosity, water absorption and dry unit weight. Thermal conductivity and Scanning electron microscope (SEM) observations of 28-day mortar specimens were also evaluated. The response surface methodology (RSM) was adopted to develop the relation between parameters and response for thermal conductivity. The test results reported that lightweight refractory and insulating mortar can be manufactured by combined use of CAC and EVP when considered strength and durability and thermal performance after high-temperature exposure. Test results also pointed out that the combined use of CAC and EVP gained significant high-temperature resistance performance in terms of compressive strength as compared to PC blended mortar specimens.

1. Introduction

The investigation of the effect of high temperature, which causes the durability problem of the buildings, on concrete and concrete building elements goes back to 1920 [1]. High temperature causes thermal dehydration of hardened cement paste or concrete, reducing the expected service life of the structure because of the permanent damage. Thus, it has become an important issue in terms of economy and safety [2–7]. With the increase in temperature in the hardened cement paste, free water is lost first, followed by the loss

* Corresponding author.
E-mail address: abenli@bingol.edu.tr (A. Benli).

https://doi.org/10.1016/j.cscm.2021.e00709
Received 21 June 2021; Received in revised form 9 September 2021; Accepted 20 September 2021
Available online 23 September 2021

of physically absorbed water and finally the chemical bond water of the hydration products is lost. On the other hand, it creates micro-cracks that cause a decrease in the strength of the concrete because of the shrinkage of the cement paste in the concrete structure and the expansion of the aggregate grains. Dehydration of slaked lime in cement paste at higher temperatures or physical/chemical transformations in aggregate cause more strength losses [8]. The main factors affecting the strength of mortars/concrete after high temperatures are: material properties and environmental factors. The mineralogy and porosity of aggregate appear to have a notable effect on the performance of concrete/mortar after high-temperature exposure. The characteristics of cement paste, aggregate and bond between aggregate and cement paste and their thermal compatibility greatly affect the strength of concrete. Moreover, environmental factors affecting the heat resistance of cement-based materials are heating rate, cooling rate, maximum exposure time, and humidity regime and loading conditions [7,9,10]. Calcium silicate hydrate (CSH) water in the interlayer and some of the combined water from CSH and sulfoaluminate hydrates will vaporize under high temperature of about 300 °C. Microcracks occur first in the $Ca(OH)_2$ concentration region at about 300 °C and then in areas of anhydrous grain at 400 °C [11]. At temperatures between 400 and 600 °C, it can activate a series of reactions, starting with the complete drying of the pore system in the hardened cement paste, CSH gel destruction and hydration product decomposition. It is possible to take preventive measures to minimize heat, such as the right material and binder selection and appropriate insulation methods. Recently, there has been an increasing trend of developing high-temperature resistant building materials for use in buildings. Calcium aluminate cement (CAC) as binder and vermiculite as a mineral additive or as aggregates can be used in mortars/concrete to minimize the effect of high temperature.

CAC is a versatile specialty cement that is advantageously used in some special applications such as monolithic refractories, foundries, furnaces and fireplaces, quick repair mortars, ceramic adhesives and sealants. The main special properties of CAC are rapid strength development, good resistance to sulfate, improved resistance to abrasion, and the ability to withstand repeated heating to high temperatures. It develops about 80% of its ultimate strength just 24 h after the start of hydration. Due to its fast hydration property, CAC is useful for low-temperature applications [12–19].

Khaliq and Khan [16] studied CAC concrete exposed to temperatures of 23, 200, 400, 600 and 800 °C as compared to PC concrete, they pointed out CAC concrete indicated a lower loss of compressive strength compared to PC concrete below 600 °C, but at higher temperatures, both materials showed similar strength deterioration. CAC concrete performed worse performance in terms of the elastic modulus as compared to PC concrete below 400 °C due to the increase in porosity. But, at 600 and 800 °C, significant improvements of 32% and 44% was obtained for CAC concrete respectively due to the higher alumina content in the CACs.

Terzic et al. [20] investigated the performances of vermiculite and perlite-based thermal insulation lightweight concretes. They found that the investigated lightweight concretes could be used both as thermal insulators and structural materials, despite decreased compressive strength after exposure to high temperatures. Roig-Flores et al. [21] focused on the development of thermo-mechanical properties of concrete with CAC and special aggregates for energy storage. They showed that the main changes mostly occur after the first thermal cycle and stabilize during successive thermal cycles with only a slight decrease in thermo-mechanical properties. Lee et al. [22] studied microstructural investigation of CAC-based ultra-high performance concrete at high temperatures. They pointed out that calcium aluminosilicate (C-A-S) gel formation was observed as a result of sintering of anhydrous CAC and anhydrous C-A-(S)-H with adjacent micro silica contributed to the residual strength after exposure to 800 °C. Baradaran-Nasiri and Nematzadeh [23] investigated the effect of high temperatures on the mechanical properties of fine recycled refractory brick aggregate and aluminate cement concrete. They showed that refractory brick aggregate and CAC increased the residual strength of concrete by twice the temperature of 800 °C. Mo et al. [24] developed a lightweight aggregate mortar skin layer for an innovative sandwich concrete composite. They highlighted that CAC mortar had better high-temperature resistance than OPC mortar. Akçaözoğlu and Akçaözoğlu [25] focused the effect of high temperature on lightweight concrete produced with expanded clay aggregate and CAC. They reported that the difference between the strength values of fast and slow cooling specimens was not significant for the CAC mixture.

Vermiculite is a mineral composed of hydrated aluminum and magnesium silicate with a naturally occurring composition that expands 8–30 times with respect to its original thickness after heating to exfoliate. Expanded vermiculite (EV) has low density, comparatively high refractoriness, chemical inertness, high fire resistance, low thermal conductivity and strong sound absorption making EV a satisfactory material for thermal and acoustics [6,7,26–28]. Concrete or mortars produced with aggregates such as expanded vermiculite, perlite, expanded clay, foamed slag and pumice with low thermal conductivity have better fire resistance and high resistance to volume expansion and decomposition and are more resistant to fire than regular concrete [3,6,7,26–39]. Koksal et al. [26] studied the characteristics of lightweight mortars with EV and silica fume under high temperatures. They noted that thermal performance enhancement of 58.2% was obtained and using vermiculite as aggregate showed good mechanical strength performance to elevated temperature. There have been very limited studies about combining CAC and EVP in concrete or mortar exposed to high temperatures in the literature. This study covers the investigation of the resistance of the mortars to be produced by replacing fine aggregate with expanded vermiculite powder (EVP) in certain proportions against high temperatures. In the mortar mixes, two different cement types namely, Portland cement (PC) and calcium aluminate cement (CAC) were used as a binder and fine aggregates were replaced with EVP at the rates of 0%, 15%, 30% and 45%. The microstructure, mechanical properties and durability of PC and CAC mortars produced in this way were determined under laboratory conditions after applying standard curing for 28 days and after the ambient and high temperature of 20 °C, 300 °C, 600 °C and 900 °C. Mechanical performance of mortar mixtures was evaluated based on compressive strength, flexural strength and UPV. The durability of the specimens was also determined using porosity, water absorption and dry unit weight. SEM observations and thermal conductivity of 28-day mortar specimens were also investigated at all these temperature ranges.

This study aimed to manufacture and evaluate low density, lightweight refractory and insulating mortars containing PC and CAC as binder and EVP as filler in different weight ratios for constructing greener buildings at different temperatures and not to use as a material for structural purposes.

2. Materials and methods

2.1. Materials used

2.1.1. Binders

Two cement types namely, CEM I 42.5R Type cement (PC) and calcium aluminate cement (CAC) with specific gravities of 3.08 and 3.20 and specific surface of 3088 and 3053 cm^2/g, respectively were used within the scope of the study. The Chemical, mechanical and physical properties of PC and CAC are demonstrated in Table 1.

2.1.2. Expanded vermiculite powder (EVP)

Ukrainian origin of expanded vermiculite (EV) was ground to obtain powder form EVP whose density was 1.68 g $/cm^3$. Table 2 exhibits the chemical composition of EVP. Fig. 1 gives the SEM images of EV and EVP, it also shows the XRD pattern and thermal gravimetric analysis (TGA) result of EVP. As seen from the SEM images of EV and EVP, EV lost accordion-shaped structure when ground and turned into separately leaf-shaped in the powder form with a maximum leaf size of about 25 μm. When the XRD pattern of the EVP is considered, it seems that EVP contains phlogopite mica and hydrobiotite phases. When TGA of EVP is considered, EVP loses about 7% of total weight at 1000 °C. The physically absorbed water is lost at about 100 °C by the dehydration of vermiculite. The chemically absorbed water is lost between 500 and 900 °C, which results in mass losses.

2.1.3. Aggregate

Crushed sand and expanded vermiculite powder were used as aggregates in the study. In the mortar production, 0–4 mm crushed sand with a specific gravity of 2.63 and a water absorption rate of 0.98% was used as fine aggregate. Gradation of sand and EVP is given in Fig. 2a. Fig. 2b–c shows expanded vermiculite and expanded vermiculite powder.

2.2. Mixture proportions and production

Mortar specimens were produced with two different cement mixtures (PC and CAC) with water/cement (w/c) ratio of 0.5 for control specimens and EVP/sand ratio of 0%, 15%, 30% and 45%. The samples were produced by taking the reference temperature (laboratory temperature) and 3 different elevated temperature values for each mortar sample. Mixing ratios are given in Table 3. While preparing the mixture, cement and aggregate were stirred first. And then, vermiculite was added and stirred again to achieve a homogeneous distribution. Then the mixing water was added. In all PC and CAC mortar mixtures, the sand is substituted with EVP at dosages of 0%, 15%, 30% and 45% by volume. The mortar specimens of 40 × 40 × 160 mm sizes are tested for mechanical and durability characteristics at 20 °C, 300 °C, 600 °C and 900 °C. After 28 days of water curing, mortar specimens were put in an oven to subject the temperature of 300 °C, 600 °C and 900 °C. The rate of temperature was selected as 7 ± 3 °C / min as proposed in the literature. After reaching the target temperature, the specimens were kept for 3 h then left for cooling at the lab.

2.3. Testing procedures

The fresh mortars were subjected to flow table test as per ASTM C1437–15 [40]. The durability characteristics of mortar/concrete can be measured by transport properties indirectly. The test on the specimens of 50 × 50 × 50 mm was executed to assess the transport properties in compliance with ASTM C642 [41] to determine the water absorption and porosity and unit weight being exposed to the room and high temperature of 300 °C, 600 °C and 900 °C. Mortar prisms of 40 × 40 × 160 mm were cast for flexural as per ASTM C348–19 [42] and compressive strength tests as per the guideline of ASTM C349–18 [43]. Three specimens were used for performing flexural strength and six specimens obtained from the flexural test were utilized for performing compressive strength at ambient conditions and after being subjected to temperature of 300 °C, 600 °C and 900 °C. UPV measurement was made to assess the quality of concretes in compliance with ASTM C597-02 [44] after being exposed to related temperatures. The thermal conductivity of the specimens was measured in a conductivity analyzer according to ASTM D7984 - 16 [45]. The response surface methodology (RSM), a

Table 1
PC and CAC properties.

Oxides%	PC	CAC	Physical properties	PC	CAC
CaO	62.09	36.41	32 μm sieve passing (%)	18.55	37.75
SiO_2	18.44	4.72	45 μm sieve passing (%)	8.12	28.86
Al_2O_3	5.50	36.56	Specific gravity (g/cm^3)	3.08	3.20
Fe_2O_3	3.18	17.10	Surface area (Blaine,cm^2/g)	3088	3053
SO_3	3.64	–	Initial /final setting time (min.)	166/216	
TiO_2	–	2.36	6 h compressive strength		47 MPa
MgO	2.24	1.26	24-h compressive strength		70 MPa
K_2O	1.06	0.13			
Na_2O	0.12	0.24			
Insoluble content	0.39	1.08			
Loss in ignition	3.34	0.14			

Table 2
Chemical composition of EVP (%).

Oxides%	EVP
SiO_2	38.76
Al_2O_3	15.89
Fe_2O_3	12.06
CaO	2.32
MgO	17.69
SO_3	0.38
K_2O	5.50
Na_2O	0.30

statistical experimental design method, was adopted to develop the relationships between parameters and response for thermal conductivity. A package program (Design-Expert) was used to response surface regression analysis.

3. Results and discussion

3.1. Evaluation of the consistency of the fresh mortars

For the evaluation of the consistency of the mortars, flow table test was carried out on fresh mortars. The flow diameter values were kept as fixed between 15 and 16 cm.

3.2. Compressive strength

The results obtained for the compressive strengths of 28-day mortar specimens upon exposure to temperatures ranging from ambient to 600 °C are shown in Fig. 3. Fig. 3b demonstrates the compressive enhancements and reductions strength in the temperature of 300 °C and 600° C. As shown, the compressive strength of PC blended mortars are higher than those of CAC blended mortars for control and all EVP incorporated specimens. It should be noted that the hydration of CAC is completely different from that of PC. In addition, an effect is known as "conversion" is known in CAC chemistry. This effect shows that the porosity of hardened CAC increases over time, resulting in a decline in strength [46]. The mortar specimens produced from PC as binder and EVP as sand replacement indicated the compressive strength varying from 48.30 to 13.90 MPa at 20 °C. As expected, the highest strength of 48.3 MPa was obtained for the PC_Control specimen and with the inclusion of EVP, compressive strength decreased to the lowest value of 13.9 MPa at 45%EVP content by 71.22% reduction as compared to PC_Control specimen. The mortar specimens produced from CAC as binder and EVP as sand replacement exhibited the compressive strength varied from 20.70 to 6.70 MPa at 20 °C. Similarly, the highest strength of 20.70 MPa was obtained for the CAC_Control specimen and the lowest value of 6.70 MPa was obtained for the mixture with 45%EVP content by 67.63% reduction in comparison with CAC_Control. The strength reduction can be attributed to the increasing porosity and decreasing unit weight values with EVP content. Another reason for the compressive strength decrease may be related to the greater demand for water required for EVP blends to complete the hydration process that produces a dried blend that causes a reduction in strength [3,6,28,38]. Strength reductions of PC blended mixtures with the inclusion EVP were 39.54% and 57.34% at 15% and 30% EVP contents, respectively. On the other hand, Strength reductions of CAC blended mixtures with the inclusion EVP were 20.28% and 48.89% at the contents of 15% and 30% EVP respectively. As seen, with the inclusion of EVP, the strength reduction of CAC blended specimens were lower than that of PC blended specimen.

After mortar specimens were exposed to high temperatures of 300 °C, 600 °C and 900 °C, the compressive strength variations were shown in Fig. 3b. Since CAC and EVP are refractory materials, the inclusion of EVP as sand replacement increased the high-temperature performance of both PC and CAC blended mortar specimens at 300 °C and 600 °C. At 300 °C, combined use of CAC and EVP showed very high performance after high-temperature exposure by strength enhancements of 64.3%, 37.6%, 30.4% and 10.5% for the mixtures of CAC control and CAC blended mortars with 15%, 30% and 45%EVP contents respectively. The strength enhancement can be due to the reactions during a temperature rise, as the porous nature of these mortars aids in steam or liquid circulation [47]. At 600 °C, CAC blended specimens exhibited strength reductions of 20.8%, 15.2%, 25.0% and 22.4% for 0, 15%, 30% and 45% EVP addition. On the other hand, PC blended specimens revealed strength reduction at all temperature ranges and higher reduction than CAC specimens. Only PC blended mortar with 45% EVP had a strength increase at 300 °C. This strength improvement may be associated with lower thermal expansion of EVP at high temperature, which prevents the penetration of heat and flame through the matrix barrier during high-temperature exposure, greatly reducing the size and number of cracks [48]. Another possible reason for increasing high-temperature resistance is that the EVP particles are granular aggregates with multiple air pockets. These air gaps act as an insulator that lowers harmful heat transfer due to high temperature [34,35,49]. Similar results were obtained by Khaliq and Khan [16]. They pointed out that concrete produced from CAC showed higher compressive toughness than normal concrete and low cracking with fewer color changes compared to NC as obtained from visual investigations after high temperature. It was observed that the combined use of CAC and EVP gained significant high-temperature resistance performance in terms of compressive strength as compared to PC blended mortar specimens. After 900 °C, all specimens completely deteriorated. So, the results of 900 °C are missing in the figures.

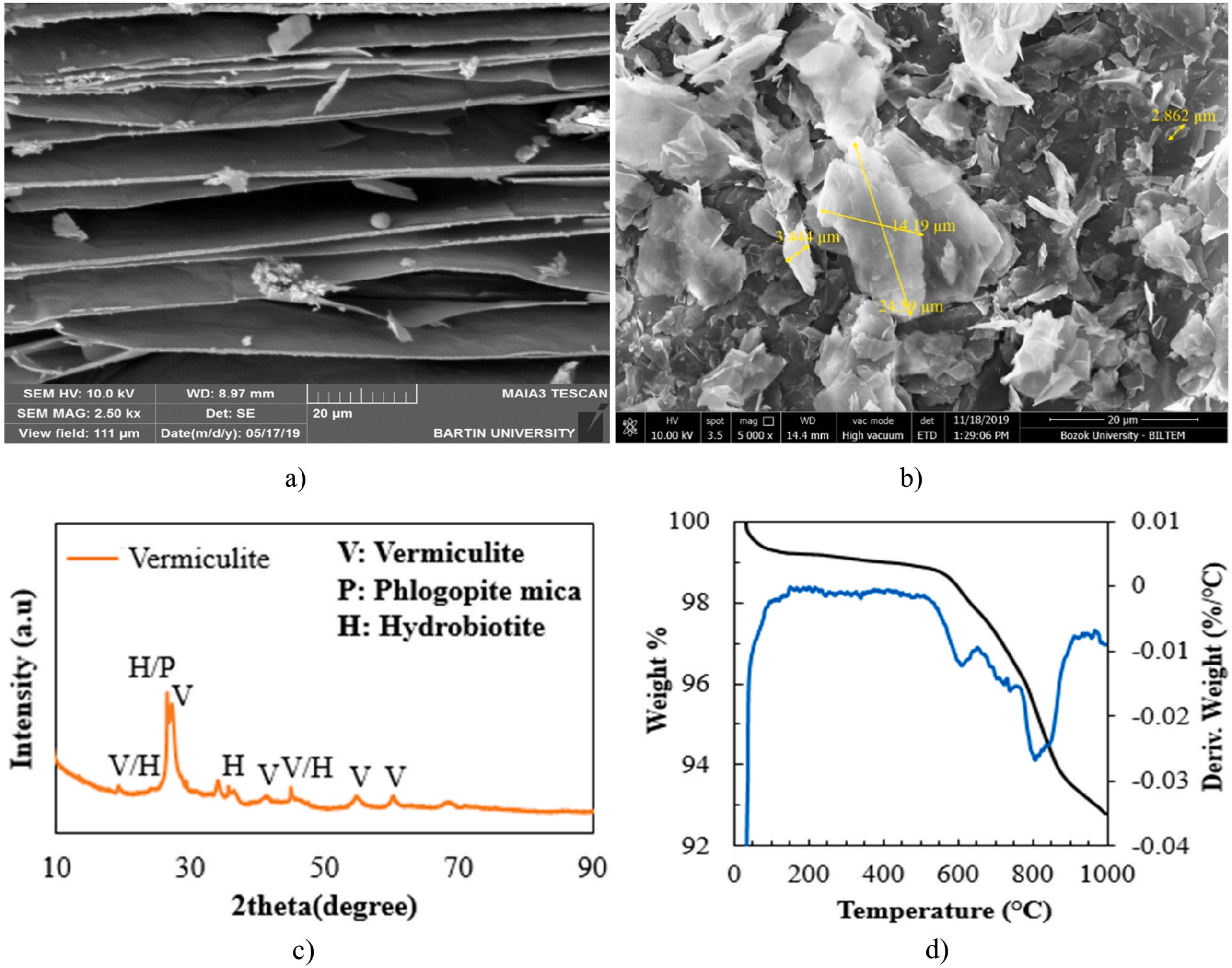

Fig. 1. a) SEM of EV b) SEM of EVP c) XRD pattern of EVP d) TGA result of EVP [26–28,38].

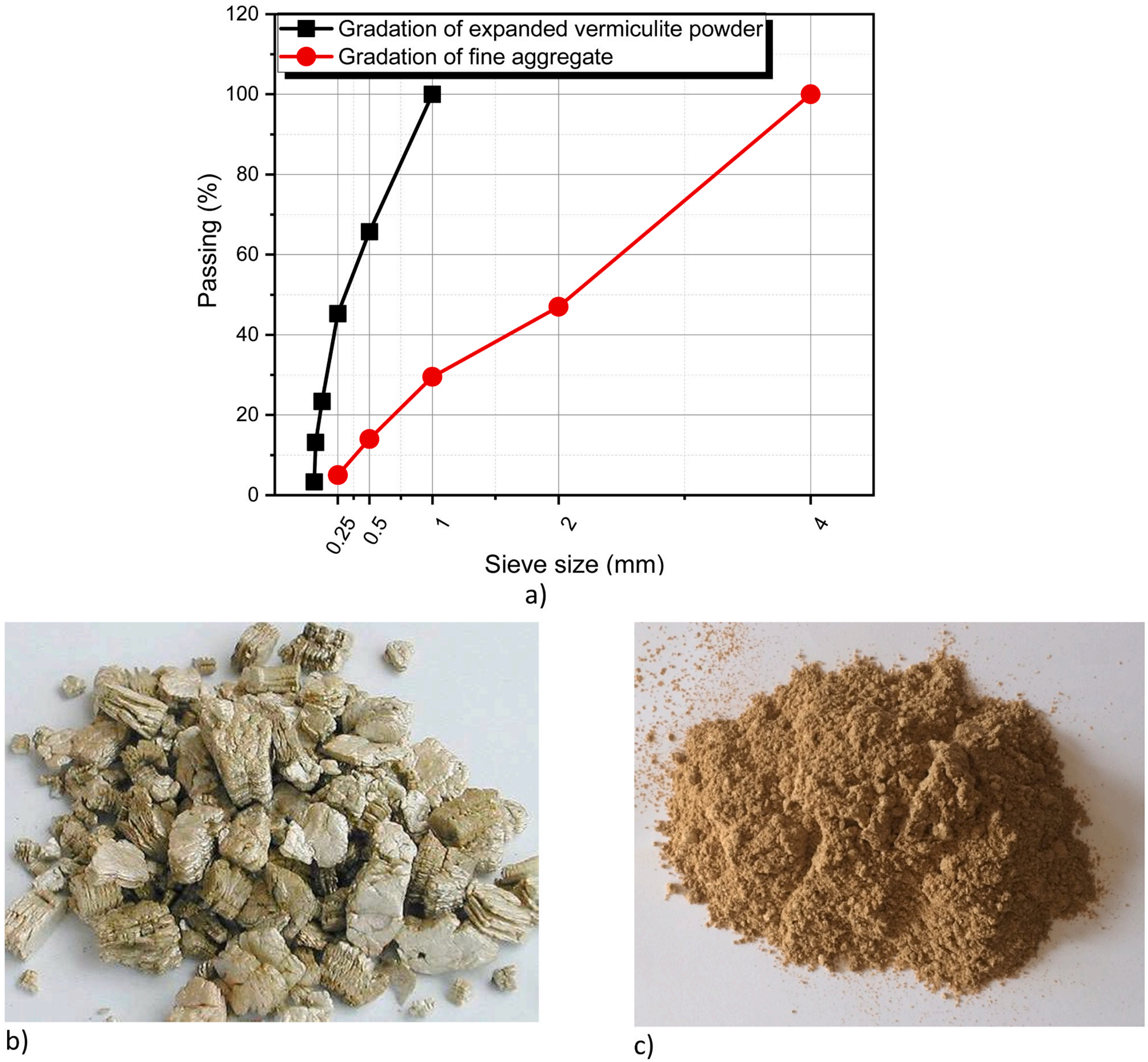

Fig. 2. a) Gradation of crushed sand and EVP b) EV c) EVP.

Table 3
Mortar mixture proportions for portland and aluminate cements.

Mix code	EVP/Sand (by volume)	Cement (g)	Water (g)	Sand (g)	EVP (g)
PC_Control	0	1350	675	4050	0
PC_EVP15	15	1350	887	3444	75
PC_EVP30	30	1350	1052	2838	150
PC_EVP45	45	1350	1237	2241	225
CAC_Control	0	1350	675	4050	0
CAC_EVP15	15	1350	887	3444	75
CAC_EVP30	30	1350	1052	2838	150
CAC_EVP45	45	1350	1237	2241	225

3.3. Flexural strength

The results obtained for the flexural strengths of 28-day mortar specimens upon exposure to temperatures ranging from ambient to 600 °C are shown in Fig. 4. Fig. 4b represents the flexural strength increase and declines in the temperature of 300 °C and 600° C. As shown, Similar to compressive strength results, PC blended mortars showed higher flexural strength than those of CAC blended mortars for control and all EVP incorporated specimens at ambient temperature. The mortar specimens produced from PC as binder and EVP as sand replacement exhibited the flexural strength varying from 6.6 to 1.9 MPa at 20 °C. As expected, the highest strength of 6.6 MPa was obtained for the PC_Control specimen and with the addition of EVP, the flexural strength decreased to the lowest value of 1.9 MPa by 71.21% reduction as compared to PC_Control specimen at 45%EVP content. The mortar specimens produced from CAC and EVP represented the flexural strength varied from 3.3 to 1.2 MPa at 20 °C. Similarly, the CAC control specimen showed the highest strength of 3.3 MPa and the lowest value of 1.2 MPa was obtained for the mixture with 45%EVP by 63.63% reduction compared to CAC control. 27.27% and 48.48% of flexural strength reductions of PC blended mixtures with the inclusion EVP were obtained at the contents of 15% and 30% EVP respectively. On the other hand, Strength reductions of CAC blended mixtures with the inclusion EVP were 0% and 33.33% at the contents of 15% and 30% EVP respectively. The strength reduction of CAC blended specimens was lower than that of PC blended specimens with EVP inclusion. The same reasons that affected the compressive strength reduction also caused the flexural strength reduction mainly due to increased porosity and water demand with EVP. The flexural strength variations were plotted in Fig. 4b after high-temperature exposure of 300 °C, 600 °C and 900 °C. For PC blended specimens, increasing EVP content decreased the strength reduction at high temperature and at 45% EVP, flexural strength increased by 42.10% at 300 °C and decreased by 47.37%, which was the lowest reduction as shown in Fig. 4b. Combined use of CAC and EVP enhanced the high-temperature resistance of mortars remarkably with strength enhancement of 63.63%, 6.06%, 18.18% and 16.67% at 300 °C and strength reduction of 24.24%, 48.48%, 54.54% and 41.67% at 600 °C for EVP content of 15%, 30% and 45% respectively. The reason for this strength enhancement can be due to low cracking [16]. It was reported that combined use of CAC and EVP gained significant high-temperature resistance performance in terms of flexural strength as compared to PC blended mortar specimens. After 900 °C, all specimens completely deteriorated. So, the results of 900 °C are missing in the figures.

Fig. 5a illustrates the compressive and flexural strength relation of PC and CAC specimens at expressed temperature ranges. As seen in Fig. 5a, it can be pointed out that a very strong quadratic relationship between the two parameters with R^2 of 0.99, 0.99 and 0.99 at 20 °C, 300 °C and 600 °C respectively, for PC blended samples. CAC samples also showed the nearly same relations with R^2 of 0.98, 0.99 and 0.98 at 20 °C, 300 °C and 600 °C respectively.

3.4. Evaluation of ultrasonic pulse velocity (UPV)

For assessing the quality of concrete/mortar, The UPV method is the most powerful non-destructive method [50]. The results obtained for the UPV results of 28-day mortar specimens upon exposure to temperatures ranging from ambient to 900 °C are shown in Fig. 6a. Fig. 6b presents the reductions in the UPV values in the temperature of 300 °C and 900°. Since PC blended mortar specimens showed higher compressive strength than CAC blended specimens, PC blended specimens also had higher UPV values than CAC specimens for all temperature ranges, but Since the aluminate cement samples are dispersed when taken out of the furnace at 900 °C, the amount of UPV of these samples could not be calculated. At ambient temperature, all PC and CAC specimens exhibited decreasing UPV values with increasing EVP content. 10.29%, 21.78% and 25.09% UPV reductions were obtained for the PC mixtures containing 15%, 30% and 45%EVP respectively. The CAC mixtures containing 15%, 30% and 45%EVP showed 6.95%, 16.24% and 32.46% reduction respectively. The reductions in the UPV values were plotted in Fig. 6b after high-temperature exposure of 300 °C, 600 °C and 900 °C. Decreasing reduction rate in UPV was observed for both PC and CAC blended mixtures as EVP content increases. More reduction in UPV was observed for CAC specimens than PC specimens.18.27%, 13.63%, 13.56% and 10.33% reduction for PC blended mixtures were obtained at 300 °C compared to PC control specimen. CAC blended mixtures showed 29.11%, 17.99%, 17.62% and 10.08% reductions at 300 °C. After 600 °C, 51.42%, 48.26%, 42.42% and 39.17% reductions for PC specimens, 72.04%, 56.02%, 50.75% and 37.58% reductions for CAC specimens were obtained. Such a change in UPV may be due to the degradation of the CSH gel after 450 °C, which increases the air void content in the concrete and thus reduces the rate at which sound waves pass through the specimens [51].

Fig. 7 plots the compressive strength and UPV relation of PC and CAC mortar specimens at expressed temperature ranges. As shown in Fig. 7, generally a strong relation between the UPV results and compressive strength of specimens was reported with the coefficients

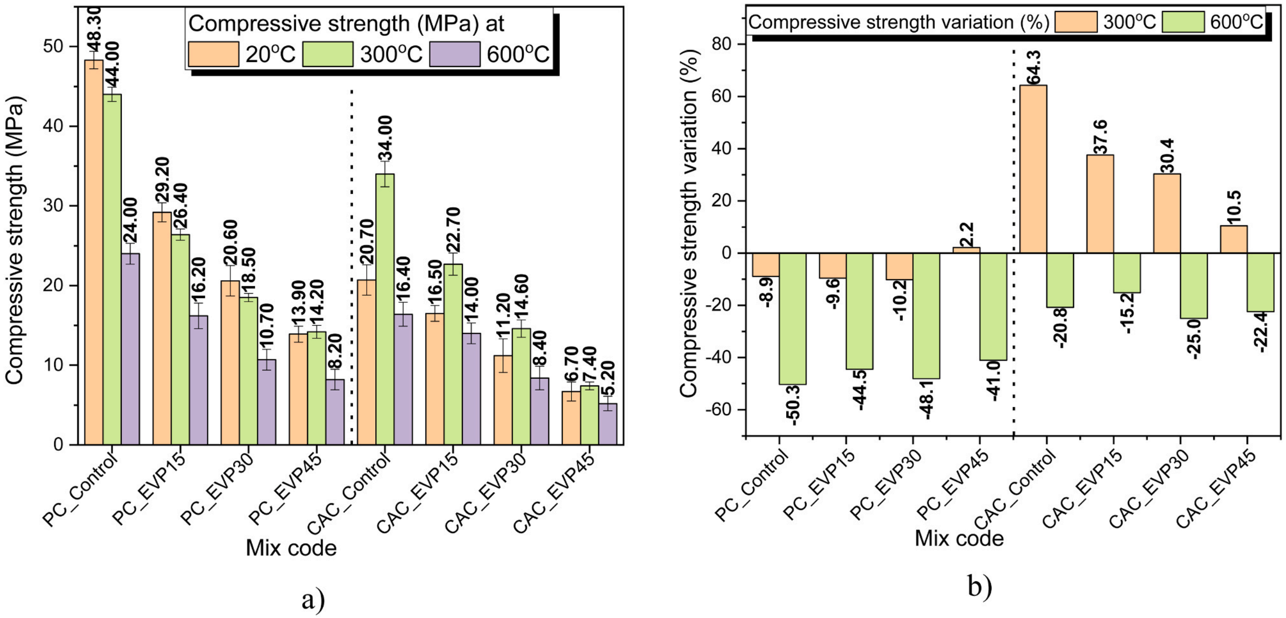

Fig. 3. a) Compressive strength and b) compressive strength variations.

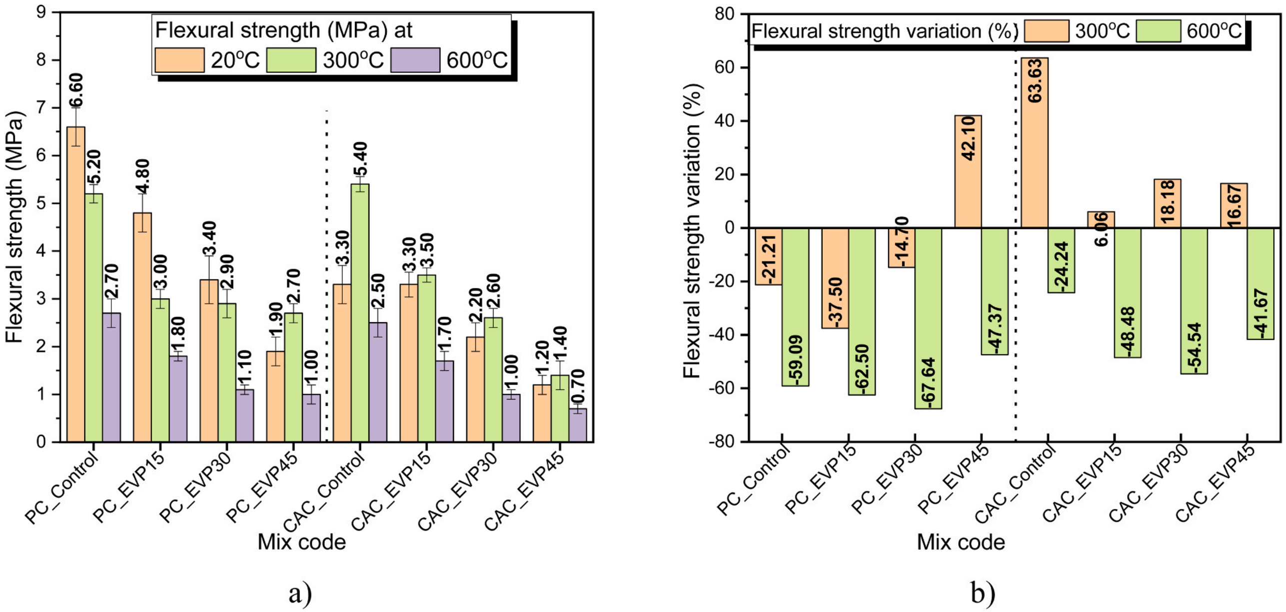

Fig. 4. a) Flexural strength and b) flexural strength variations.

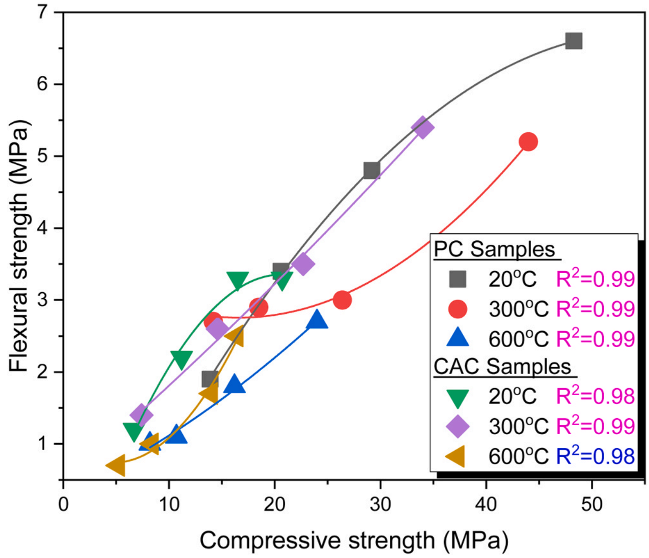

Fig. 5. The compressive -flexural strength of mortar specimens.

of correlation R^2 of 0.97, 0.94 and 0.55 at 20 °C, 300 °C and 600 °C respectively for PC blended samples and 0.99, 0.88 and 0.81 at 20 °C, 300 °C and 600 °C respectively for CAC samples. As expected, higher compressive strength was associated with higher UPV values. The correlation between the strength and UPV lowered with increasing temperature exposure, especially for PC blended mortars at 600 °C.

3.5. Evaluation of dry unit weight

The results obtained for the dry unit weight of 28-day specimens upon exposure to temperatures ranging from ambient to 600 °C are shown in Fig. 8a. Fig. 8b presents dry unit weight reductions in the temperature of 300 °C and 600° C. As shown, CAC blended specimens had higher dry unit weight than PC blended specimens due to the higher specific gravity of CAC. All PC and CAC mortar specimens exhibited decreasing dry unit weight with increasing EVP content and temperature. The PC specimens exhibited the dry unit weight varying from 2174.75 to 1672.50 kg/m^3 at 20 °C. As expected, the greatest dry unit weight of 2174.75 kg/m^3 was obtained for the PC control specimen and the dry unit weight decreased to the lowest value of 1672.50 kg/m^3 by 23.09% reduction as compared to PC control specimen at 45%EVP content. At 15% and 30% EVP contents, unit weight reductions were 6.75% and 14.11%. The CAC specimens exhibited the unit weight varying from 2280.50 to 1798 kg/m^3 at 20 °C. As expected, the greatest unit weight of 2280.50 kg/m^3 was obtained for the CAC control specimen and the dry unit weight decreased to the lowest value of 1798 kg/m^3 by 21.14% reduction compared to the CAC control specimen at 45%EVP content. At 15% and 30% EVP contents, unit weight reductions of CAC specimens were 4.82% and 12.27%. As represented in the compressive strength results, CAC specimens showed less dry unit weight reduction than PC specimens with EVP. The dry unit weight decline of EVP incorporated mortars can be due to the lower specific gravity of EVP than sand and more water needed for EVP in the fresh state and leaving the water from the mortar body in the hardened state. Fig. 8b plots the dry unit weight reductions after high-temperature exposure of 300 °C and 600 °C. As shown in Fig. 8b, PC blended specimens revealed unit weight reductions of 2.3%, 4.9%, 3.7% and 5.8% at 300 °C and 7.8%, 10.5%, 10.6% and 11.8% at 600 °C at 15%, 30% and 45% EVP replacement level respectively as compared to the dry unit weight at ambient temperature. On the other hand, CAC blended specimens revealed unit weight reductions of 1.9%, 3.2%, 4.1% and 6.5% at 300 °C and 9.6%, 10.6%, 10.8% and 14.7% at 600 °C at 15%, 30% and 45% EVP replacement level respectively as compared to the dry unit weight at ambient temperature. It seems that at 15% and 30% EVP content, at 600 °C, both PC and CAC blended specimens showed nearly the same dry unit weight reduction, but at 45%EVP, CAC showed more unit weight reduction. After 900 °C, specimens completely deteriorated. So, the results of 900 °C are missing in the figures.

Fig. 9 plots the compressive strength and unit weight relation of PC and CAC mortar specimens at expressed temperature ranges. As represented in Fig. 9, very high relation between the unit weight results and compressive strength of mortar specimens was reported with the coefficients of correlation R^2 of 0.99, 0.98 and 0.99 at 20 °C, 300 °C and 600 °C respectively for PC blended samples and 0.99, 0.99 and 0.98 at 20 °C, 300 °C and 600 °C respectively for CAC samples. As expected, higher compressive strength was associated with higher dry unit weight values.

3.6. Thermal conductivity

Thermal conductivity results of 28-day mortar specimens upon exposure to temperatures ranging from ambient to 600 °C were presented in Fig. 10. An important relationship exists between the thermal conductivity and unit weight of concrete [52,53]. It was

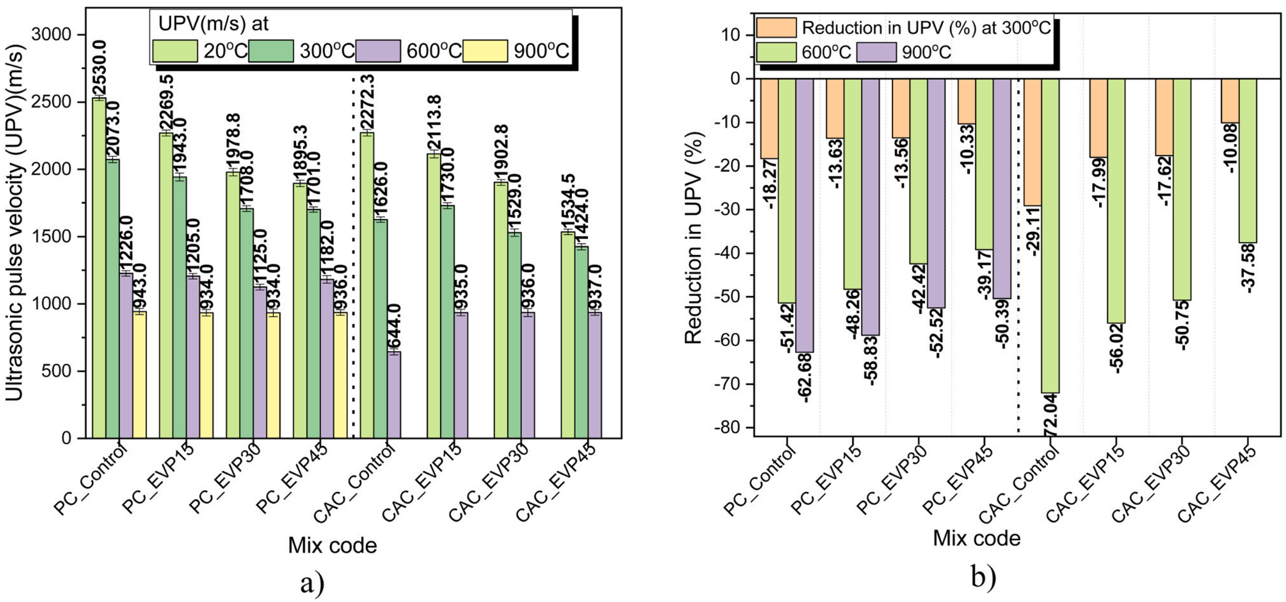

Fig. 6. a) The values of UPV and b) UPV decrease.

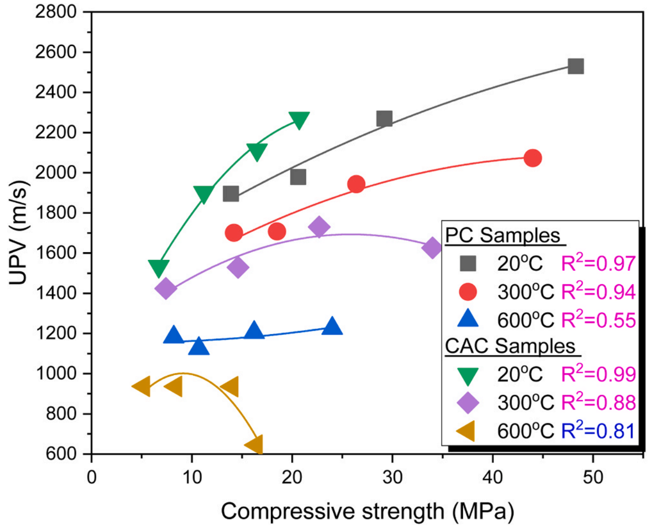

Fig. 7. The compressive strength and UPV relation of mortar specimens.

observed that CAC blended mixtures had lower thermal conductivity than PC blended mixtures. Thermal conductivity decreased by replacing sand with EVP and temperature increased. CAC blended control and 15% EVP substituted mixtures showed lower thermal conductivity than PC blended control and 15% EVP substituted mixtures. As expected, replacing sand with EVP at 15%, 30% and 45% reduced the thermal conductivity of PC blended specimens significantly by 37.46%, 55.79% and 62.85% respectively, at 20 °C due to porous structure and low density of EVP. Similarly, for CAC specimens, thermal conductivity decreased by 0.69%, 14.58% and 22% at 15%, 30% and 45% EVP content. At room temperature, CAC blended specimens had more compact and dense structure, which led to higher unit weight and lower thermal conductivity reduction than PC blended mixtures. At 300 °C, thermal conductivity reduction at 15%, 30% and 45% EVP content was 44.05%, 55.70% and 61.44% for PC blended specimens and 0.12%, 5.33% and 36.54% for CAC blended specimens respectively. The lower reduction was obtained at this temperature, similar to reduction at room temperature for CAC specimens. This means that less damage occurred in the structure of CAC specimens that PC specimens. At the temperature of 600 °C, thermal conductivity reduction at 15%, 30% and 45% EVP content was 31.03%, 67.46% and 70.63% for PC blended specimens and 9.25%, 14.78% and 68.12% for CAC blended specimens. The lower reduction was also obtained at this temperature, similar to that at room temperature for CAC specimens. This means that less damage occurred in the structure of CAC specimens than PC specimens. As represented in Fig. 10b, a very strong correlation between the unit weight results and thermal conductivity of mortar specimens was reported with the coefficients of correlation R^2 of 0.99, 0.98 and 0.97 at 20 °C, 300 °C and 600 °C respectively for PC blended samples and 0.94, 0.98 and 0.97 at 20 °C, 300 °C and 600 °C respectively for CAC samples. As expected, lower unit weight was associated with lower thermal conductivity values.

3.6.1. Response surface methodology for thermal conductivity

The response surface methodology (RSM), a statistical experimental design method, was adopted to develop the relationships between parameters and response for thermal conductivity. A package program (Design-Expert) was used to response surface regression analysis. Experimental plan of response surfaces consists of two variables (i.e. EVP/FA and T); four-level (i.e. EVP/FA = 0%, 15%, 30%, and 45% by volume) and three-level (i.e. T = 20° C, 300 °C and 600 °C) full factorial experimental design for each cement type. The experimental design scheme for the thermal conductivity is demonstrated in Fig. 11.

In each cement type, twelve experimental data for TC were fitted to a polynomial type mathematical model using variance analysis (ANOVA). Equations of the best fitting response surface models established for the thermal conductivity with Portland cement and Calcium Aluminate cement at different temperatures are obtained as follows:

For Portland cement;.

$$TC = 1{\cdot}795\text{–}0048{*}(EVP/FA) - 0{\cdot}007{*}(T) + 0{\cdot}0006((EVP/FA)^2 \tag{1}$$

For Calcium Aluminate cement;.

$$TC = 1{\cdot}172\text{–}0{\cdot}035{*}(EVP/FA) - 0{\cdot}008{*}(T) - 0{\cdot}00025{*}(EVP/FA)^2 \tag{2}$$

Response surfaces of the models are shown in Fig. 12. The coefficients of determination (R^2) of PC and CAC cement models were 0.966 and 0.939, respectively. Comparison of the experimentally obtained and predicted thermal conductivity values of mortars for each cement type is illustrated in Fig. 13.

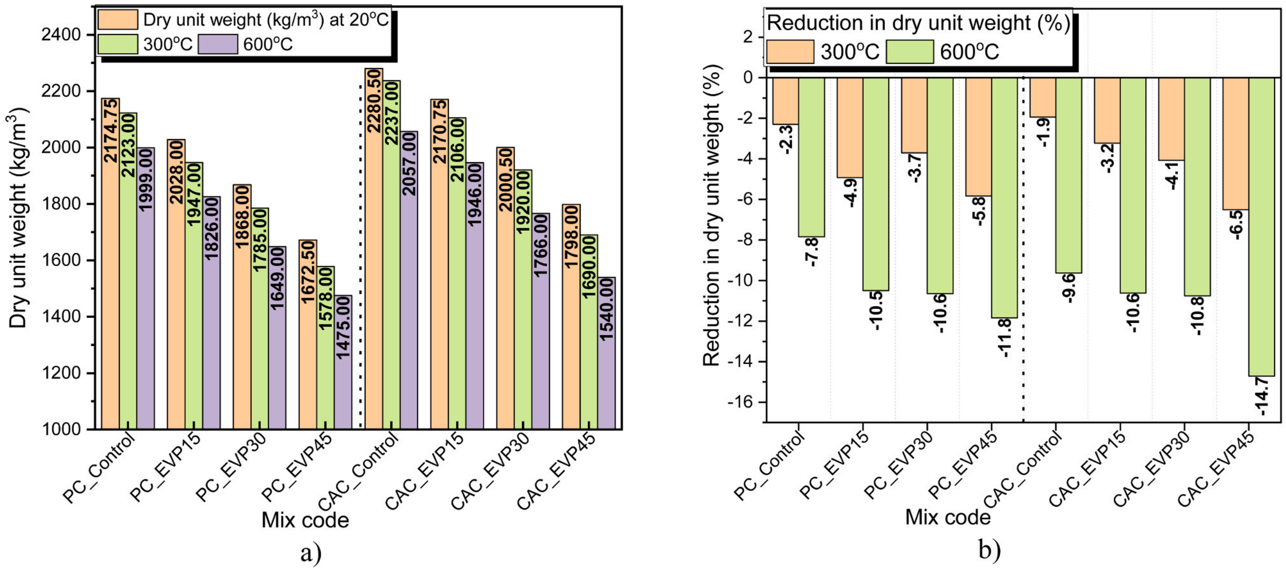

Fig. 8. a) Unit weight and b) unit weight reductions of mortar specimens.

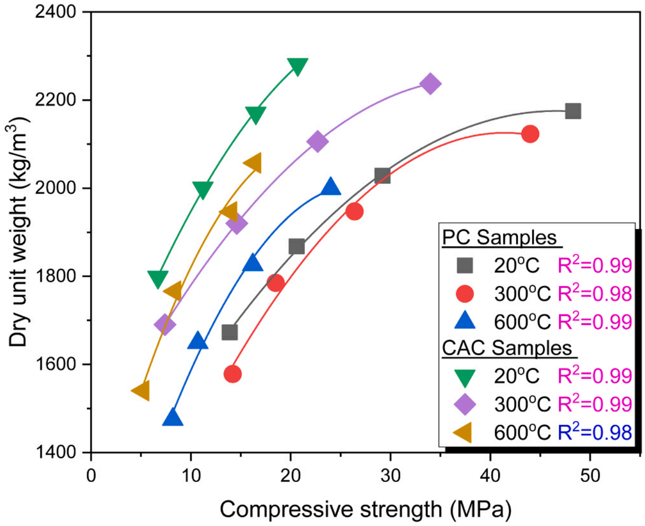

Fig. 9. The compressive strength and dry unit weight relation of mortar specimens.

3.7. Porosity

Fig. 14a represents the porosity values of EVP incorporated PC and CAC mortar mixtures at all temperature ranges. Fig. 14b demonstrates the porosity increase of specimens after being exposed to the expressed temperature ranges. The porosity of all PC and CAC mortar specimens was enhanced at all temperature ranges with the addition of EVP. The PC specimens demonstrated the porosity varying from 15.08% to 31.27% at 20 °C. The porosity enhancements of the PC mortar specimens with the addition of EVP were 31.43%, 63.85% and 107.36% at EVP contents of 15%, 30% and 45% respectively, compared with PC control specimens at ambient temperature. The CAC specimens demonstrated the porosity varying from 15.03% to 27.59% at 20 °C.The porosity enhancements of the CAC specimens with the addition of EVP were 18.76%, 53.16% and 83.56% at EVP contents of 15%, 30% and 45% respectively, compared with CAC control specimen at ambient temperature. It was obviously seen that porosity enhancements of CAC specimens were lower than those of PC specimens at ambient temperature as observed similar behavior for compressive strength. Fig. 14b plots the enhancements in the porosity after high-temperature exposure of 300 °C and 600 °C. As shown in Fig. 14b, PC blended specimens exhibited porosity enhancements of 20.01%, 44.98%, 22.21% and 26.44% at 300 °C and 62.74%, 80.36%, 54.20% and 50.64% at 600 °C at 15%, 30% and 45% EVP replacement level respectively as compared to the porosity value at ambient temperature. On the other hand, CAC blended specimens revealed porosity enhancements of 19.30%, 30.68%, 29.56% and 37.04% at 300 °C and 85.86%, 94.74%, 57.68% and 80.55% at 600 °C as compared to the porosity value at ambient temperature. The porous nature and lower fine particles of EVP resulted in enhancements in the porosity [54]. PC blended mortar had lower porosity, especially at 45% EVP replacement level than CAC blended mortar specimens at 600 °C temperature exposure. After 900 °C, all specimens completely deteriorated. So, the results of 900 °C are missing in the figures.

Fig. 15a plots PC and CAC mortar specimens' compressive strength and porosity relation at expressed temperature ranges. As shown in Fig. 15, a very high relationship between the porosity and compressive strength of specimens was reported with the coefficients of correlation R^2 of 0.99, 0.99 and 0.99 at 20 °C, 300 °C and 600 °C respectively for PC blended samples and 0.99, 0.99 and 0.98 at 20 °C, 300 °C and 600 °C respectively for CAC samples. As expected, higher compressive strength was associated with lower porosity values. Fig. 15b plots the unit weight and the porosity relationship of PC and CAC mortar specimens at all temperature ranges. As shown in Fig. 11b, a very high relationship between unit weight and the porosity of mortar specimens was also reported with the coefficients of correlation R^2 of 0.99, 1.00 and 0.99 at 20 °C, 300 °C and 600 °C respectively for PC blended samples and 0.99, 0.99 and 1.00 at 20 °C, 300 °C and 600 °C respectively for CAC samples. As expected, higher porosity was associated with lower dry unit weight values. Fig. 15c plots the PC and CAC mortar specimens' porosity and flexural strength relation at expressed temperature ranges. As shown in Fig. 15c, flexural strength–porosity dependence of mortar specimens was so strong that coefficients of correlation R^2 of 0.99, 0.96 and 0.99 at 20 °C, 300 °C and 600 °C respectively for PC blended samples and 0.98, 0.99 and 0.98 at 20 °C, 300 °C and 600 °C respectively for CAC samples. It can be reported that from these correlations that flexural strength strongly depends on the porosity values.

3.8. Water absorption

The results obtained for the water absorption of 28-day mortar specimens upon exposure to temperatures ranging from ambient to 600 °C are shown in Fig. 16a. Fig. 16b presents enhancements in the water absorption at the temperature of 300 °C and 600 °C. Obviously, water absorption of both PC and CAC specimens increased with increasing content of EVP and temperature due to the porous structure of EVP, as stated before. Observing Fig. 16a that CAC blended specimens mostly had lower water absorption than PC

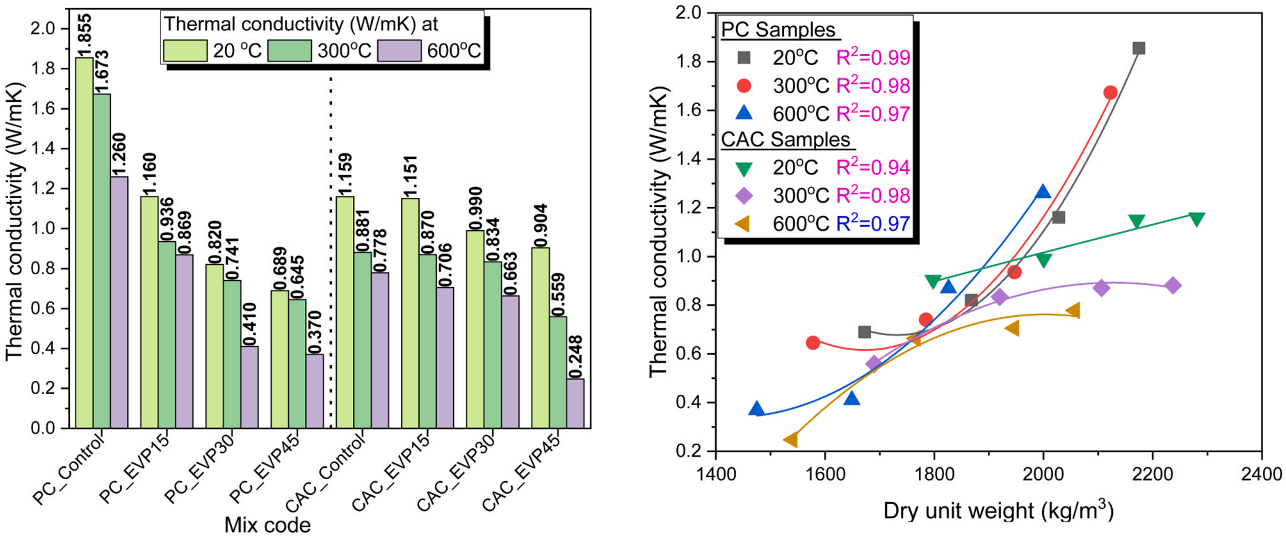

a) b)

Fig. 10. a) Thermal conductivity values and b) Dry unit weight vs. thermal conductivity.

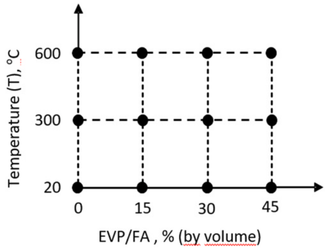

Fig. 11. Experimental design scheme.

blended specimens. The PC specimens exhibited the water absorption varying from 6.88% to 18.68% at 20 °C. As expected, the lowest water absorption of 6.88% was obtained for the PC control specimen. The water absorption increased to the highest value of 18.38% at 45%EVP content by 171.51% enhancement compared to PC control specimen. The CAC specimens exhibited water absorption varying from 6.58% to 15.35% at 20 °C. As expected, the lowest water absorption of 6.58% was obtained for the CAC control specimen. The water absorption increased to the highest value of 15.35% at 45%EVP content by 133.28% enhancement compared to the CAC control specimen. From the results, it can be concluded that CAC blended mortars with EVP showed a lower enhancement in water absorption than PC blended mortars with EVP. Similar behavior was also observed for compressive strength, CAC specimens also showed lower compressive strength reduction than PC specimens with EVP addition at room temperature. Fig. 16b presents the enhancements in the water absorption after high-temperature exposure of 300 °C and 600 °C. As shown in Fig. 12b, PC blended specimens exhibited water absorption enhancements of 23.64%, 37.79%, 36.11% and 33.33% at 300 °C and 84.73%, 89.20%, 88.28% and 72.42% at 600 °C at 15%, 30% and 45% EVP content respectively as compared to the water absorption at ambient temperature. On the other hand, CAC blended specimens revealed water absorption enhancements of 20.15%, 30.49%, 32.47% and 42.67% at 300 °C and 108.37%, 106.10%, 94.81% and 101.95% at 600 °C in comparison with the water absorption at ambient temperature. The porous nature and lower fine particles of EVP led to enhancements in the porosity and water absorption [54]. It can be reported that CAC control had the lowest water absorption increase at 300 °C and PC blended mortar containing 45% EVP showed the lowest water absorption increase at 600 °C. It seems that CAC blended mortar had a lower water absorption increase for CAC control and 15% and 30% EVP than PC blended mortar specimens at 300 °C temperature exposure. However, at 600 °C temperature exposure, CAC blended mortar had a higher water absorption increase than PC blended mortar specimens at all EVP rates. After 900 °C, specimens completely deteriorated. So, the results of 900 °C are missing in the figures.

Fig. 17 illustrates the compressive strength and the water absorption relation of PC and CAC mortar specimens at expressed temperature ranges. As seen in Fig. 17, very high relationship between the compressive strength and water absorption of mortar specimens was reported with the coefficients of correlation R^2 of 0.99, 0.98 and 0.98 at 20 °C, 300 °C and 600 °C respectively for PC blended samples and 0.99, 0.99 and 0.98 at 20 °C, 300 °C and 600 °C respectively for CAC samples. As expected, higher compressive strength was associated with lower water absorption values.

3.9. SEM observations

SEM observations of PC control and PC EVP30 (containing 30%EVP) mortar specimens with 5000X and 25000X magnification at ambient and temperatures of 300 °C and 600 °C are represented in Fig. 18. At 20 °C of PC control, SEM observations of PC control indicate a compact and dense microstructure with very tiny micro-cracks. Fig. 18 shows that after the samples were subjected to 300 °C, the internal structures showed significant changes and the decomposition of the binder with significant cracking of the cementitious matrix. Form these images, it can be observed the appearance change of CSH crystals with temperature increase. CSH crystals get thinner and slimmer with an increase in temperature, causing a decrease in compactness. At 600 °C, severe damage and the expansion of cracks in number and size can be seen from the SEM image. Chemically and physically bound water of gel-like hydration products seems to disappear in mortar samples. Important cracks are observed in the interface transition region. It is obvious that after 600 °C, hydration products are greatly damaged. After high temperatures, the C-S-H gel structure was dehydrated and the structure of the gel changed. Hydration products such as CH and CSH were observed in PC mortars at room temperature. PC mortar appears to be stable up to 300° C. Because no crack network was observed in the microstructure. However, it was determined that hydration products were damaged at 600° C. At 600° C, fibrous CSH structures could not be determined. A more round and porous structure is seen in the microstructure. The damage at 600° C is the shrinkage of the paste caused by the loss of water of the hydration products. With the increase in temperature, thermal stress increases and as a result, the micro-crack network expands. Since the porosity of PC mortars is very high, it is generally not damaged much at 300° C.SEM analysis of PC EVP30 (containing 30% EVP) mortar specimens with 5000X and 25000X magnification at ambient and temperatures of 300 °C and 600 °C are also represented in Fig. 18. At room temperature of PC with 30%EVP, SEM images show clearly that expanded vermiculite powders are homogeneously distributed within the mortar matrix containing porous and weak dense structures. When compared to PC control, it seems more voids and many porous in the matrix. Fig. 18 shows that after the samples were subjected to 300 °C, more cracks and porous formed and they enlarged. The mortar matrix exhibited significant changes and the decomposition of the binder with significant cracking. Important cracks are observed in the interface transition region. It is obvious that after 600 °C, hydration products are greatly damaged. After high temperatures, the C-S-H gel structure was dehydrated and the structure of the gel changed.

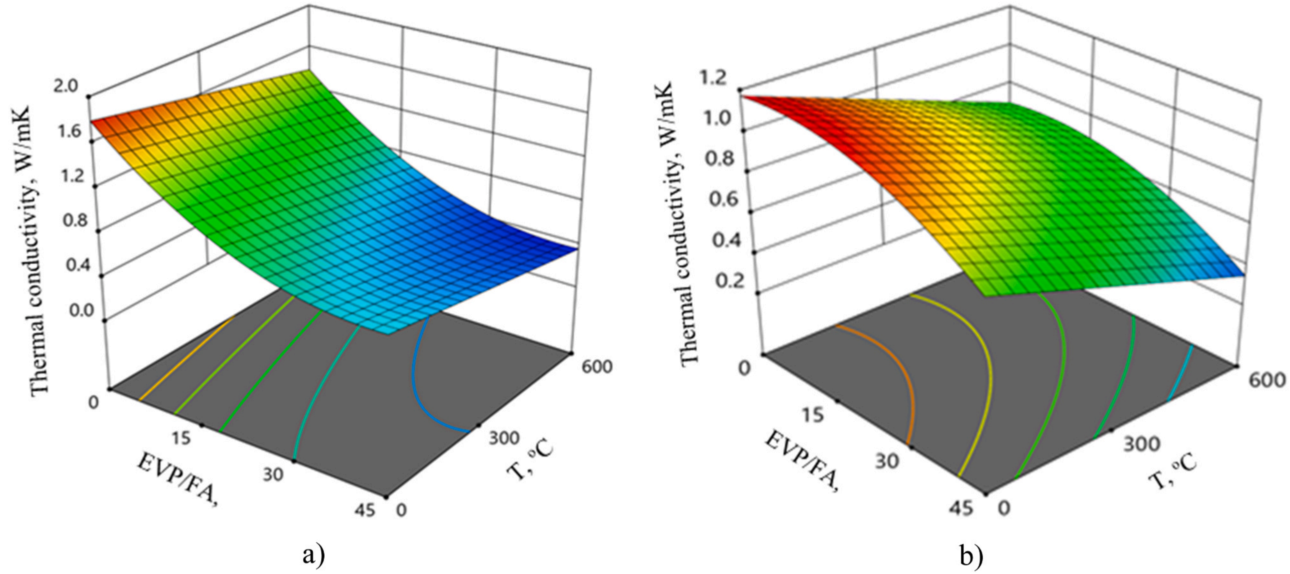

Fig. 12. Three-dimensional surface plots for thermal conductivity of a) PC and b) CAC specimens.

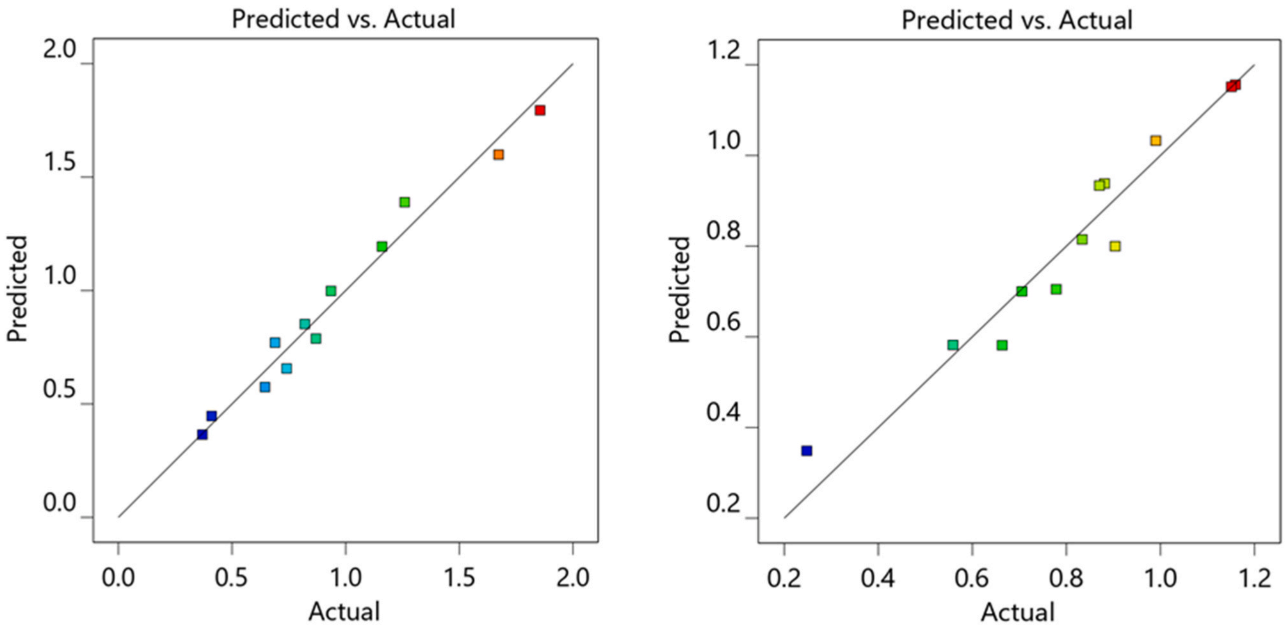

a) b)

Fig. 13. Scatter plot between target and predicted values of thermal conductivity of a) PC and b) CAC specimens.

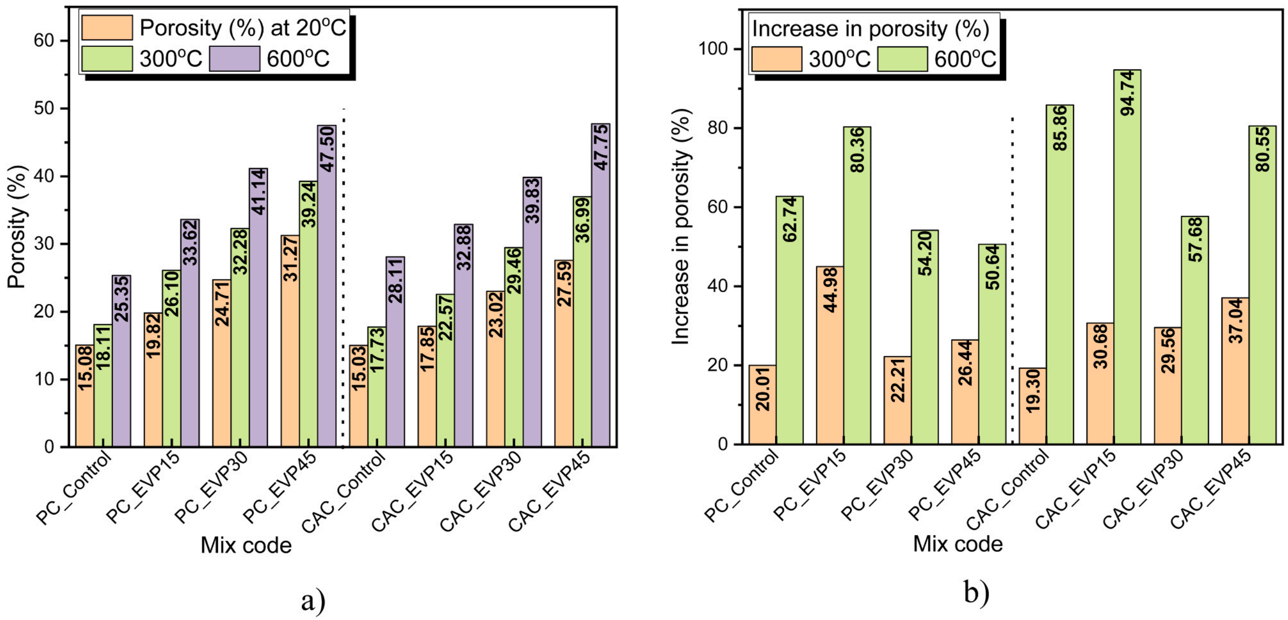

Fig. 14. a) Porosity and b) porosity change of specimens.

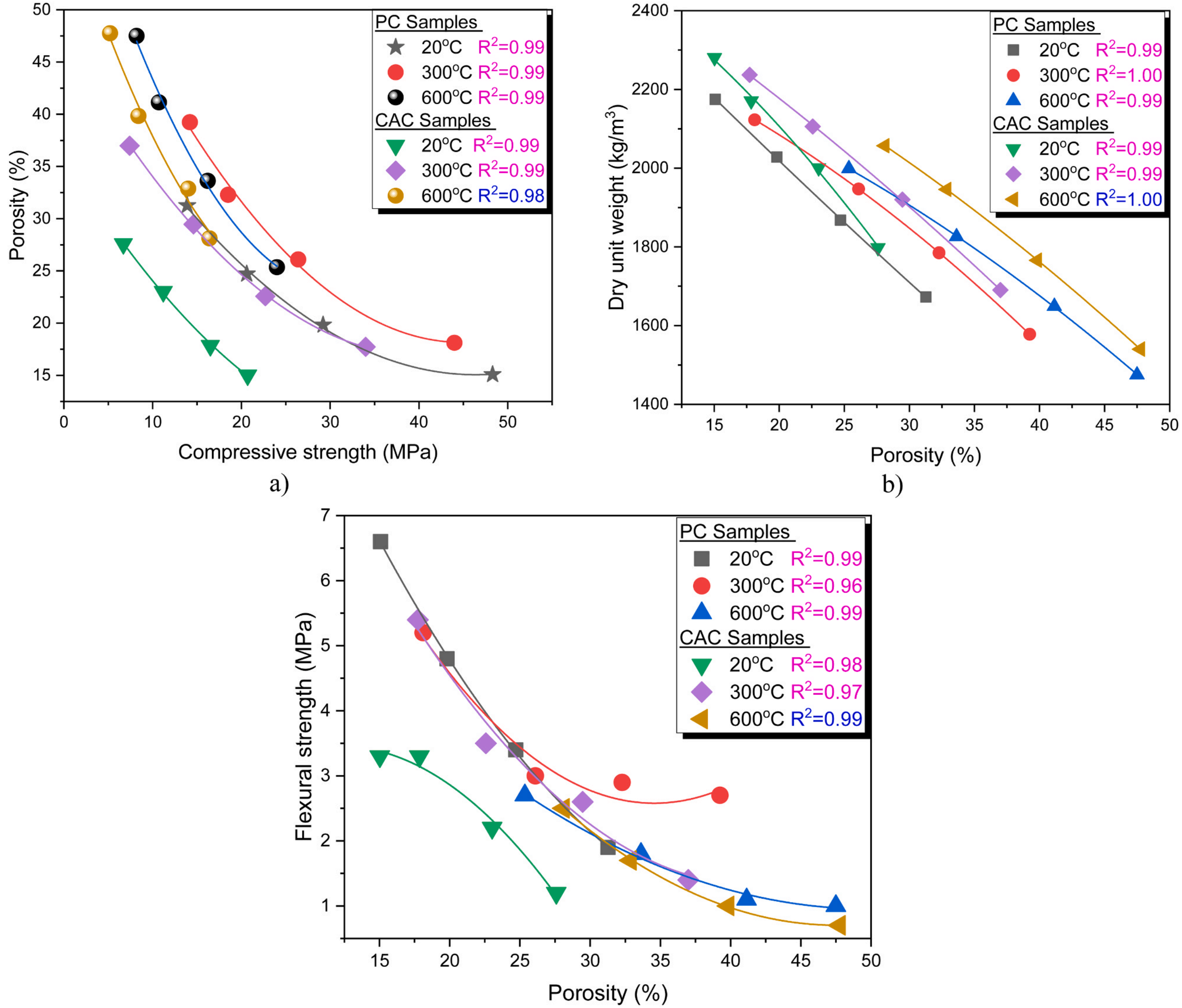

Fig. 15. a) Relation among the compressive strength & porosity and b) porosity & dry unit weight c) flexural strength–porosity dependence of mortar specimens.

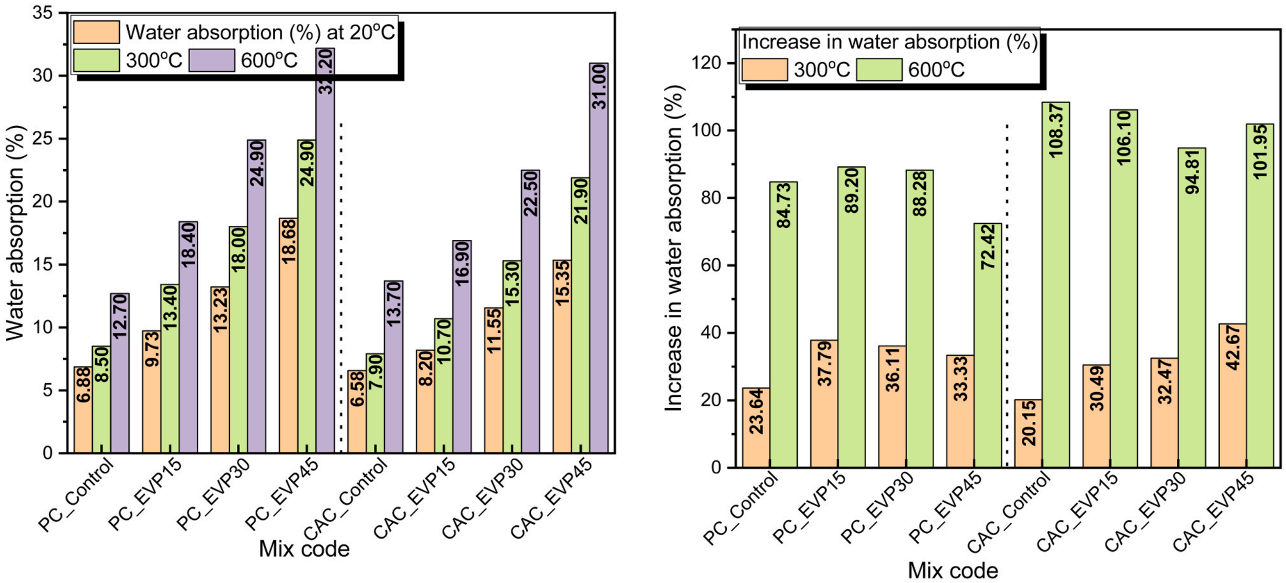

a) b)

Fig. 16. a) Values of water absorption and b) water absorption change of specimens.

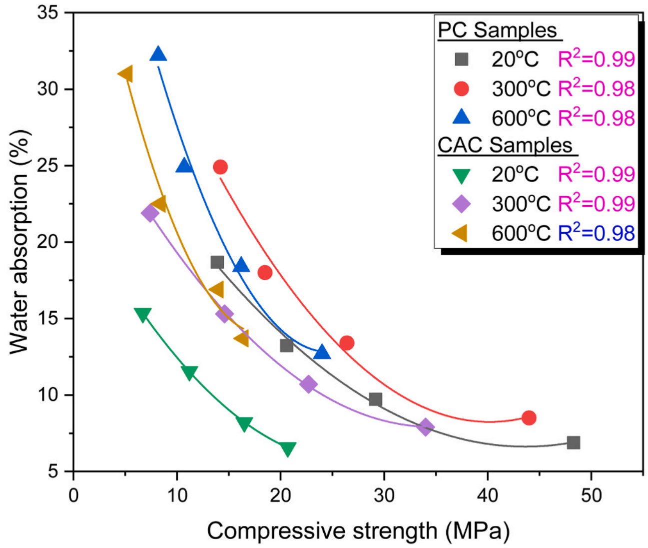

Fig. 17. Relation among the compressive strength and water absorption of mortar specimens.

Hexagonal metastable hydrate crystals of C_2AH_8 were detected in room temperature CAC mortars (Fig. 19). Morphological changes have occurred in CAC mortars as a result of the high-temperature effect. C_3AH_6 and AH_3 structures were intensely observed in CAC mortars exposed to 300 °C. A small number of cubic crystals of C_3AH_6 and AH_3 were observed in CAC mortars exposed to 600° C. Also, it was determined that the porosity increased due to the evaporation of chemical water with the effect of high temperature. However, the presence of the AH_3 gel covering the C_3AH_6 crystals enabled the microstructure to be dense at 300 °C. These hydration products also reduced the damage at 600 °C compared to PC mortars. Also, the use of EVP in CAC mortars has reduced the micro-crack network.

4. Conclusion

The investigation of the resistance of the mortars to be produced by replacing fine aggregate with expanded vermiculite powder (EVP) in certain proportions against high temperatures was performed in this study. In the mortar mixes, two different cement types namely, Portland cement (PC) and calcium aluminate cement (CAC) were used as a binder and fine aggregate (sand) was replaced with EVP. The microstructure, mechanical, thermal properties and durability of PC and CAC mortars produced in this way were determined under laboratory conditions after applying standard curing for 28 days and after being temperature exposure of 300 °C, 600 °C and 900 °C and the following conclusions have been drawn:

- The compressive strength of PC blended mortars are higher than those of CAC blended specimens for control and all EVP incorporated specimens.
- At 300 °C, combined use of CAC and EVP showed very high performance after high-temperature exposure by strength enhancements of 64.3%, 37.6%, 30.4% and 10.5% for the mixtures of CAC control and CAC blended mortars with 15%, 30% and 45%EVP contents respectively.
- At 600 °C, CAC blended specimens exhibited strength reductions of 20.8%, 15.2%, 25.0% and 22.4% for 0, 15%, 30% and 45% EVP addition. On the other hand, PC blended specimens revealed strength reduction at all temperature ranges and higher reduction than CAC specimens. Similarly, the highest strength of 20.70 MPa was obtained for the CAC_Control specimen and the lowest value of 6.70 MPa was obtained for the mixture with 45%EVP content by 67.63% reduction in comparison with CAC_Control.
- The combined use of CAC and EVP gained significant high-temperature resistance performance in terms of compressive strength as compared to PC blended mortar specimens.
- Combined use of CAC and EVP gained significant high-temperature resistance performance in terms of flexural strength compared to PC blended mortar specimens. Combined use of CAC and EVP enhanced the high-temperature resistance of mortars remarkably with strength enhancement of 63.63%, 6.06%, 18.18% and 16.67% at 300 °C and strength reduction of 24.24%, 48.48%, 54.54% and 41.67% at 600 °C for EVP content of 15%, 30% and 45% respectively.
- Since PC blended mortar specimens showed higher compressive strength than CAC blended specimens, PC blended specimens also had higher UPV values than CAC specimens for all temperature ranges.
- More reduction in UPV was observed for CAC specimens than PC specimens. After 600 °C, 51.42%, 48.26%, 42.42% and 39.17% reductions for PC specimens, 72.04%, 56.02%, 50.75% and 37.58% reductions for CAC specimens were obtained. Such a change in UPV may be due to the degradation of the CSH gel after 450 °C,
- The PC specimens exhibited lower dry unit weight than The CAC specimens

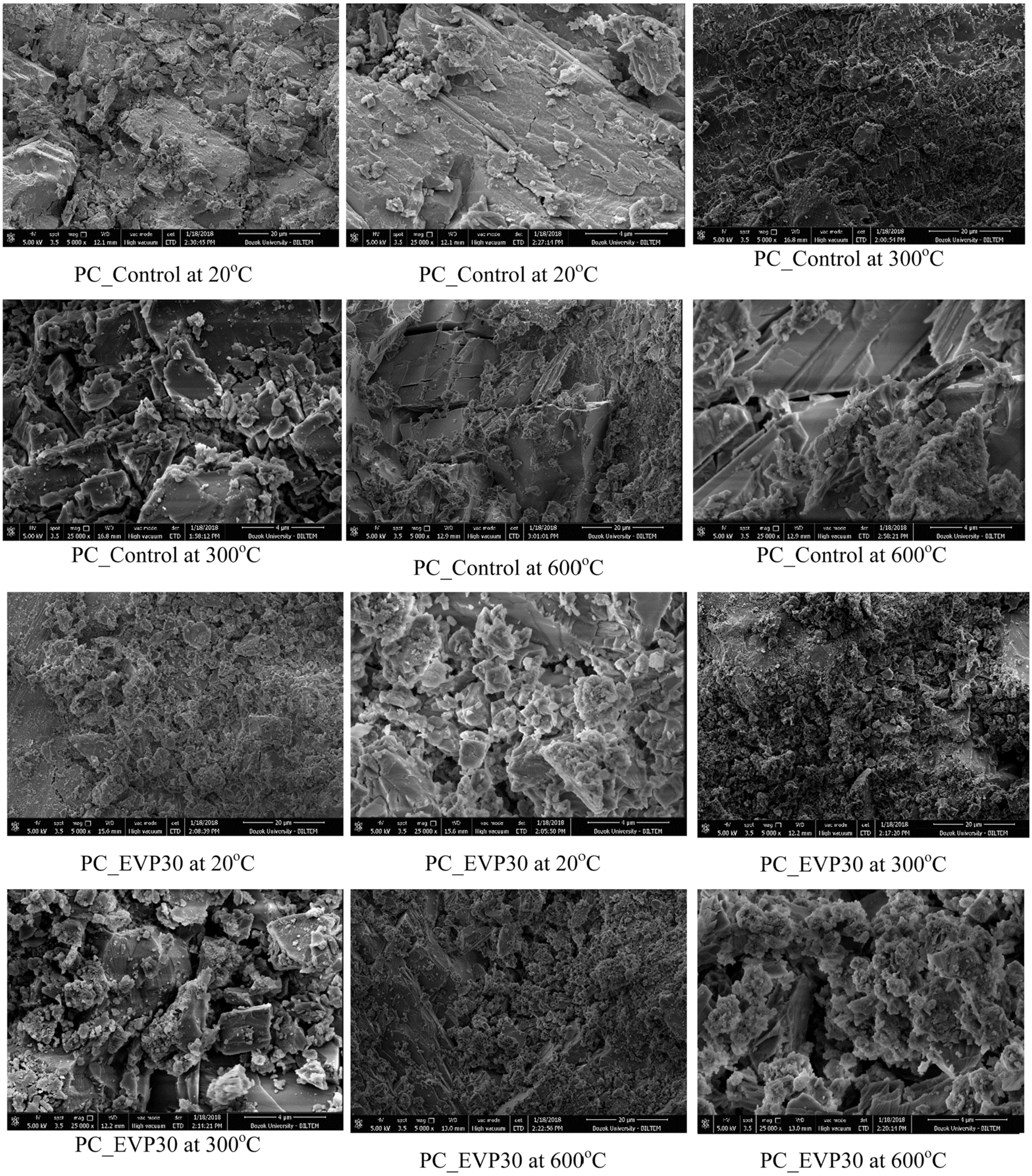

Fig. 18. SEM observations of PC control and PC EVP30 specimens after exposure to 20 °C, 300 °C and 600 °C.

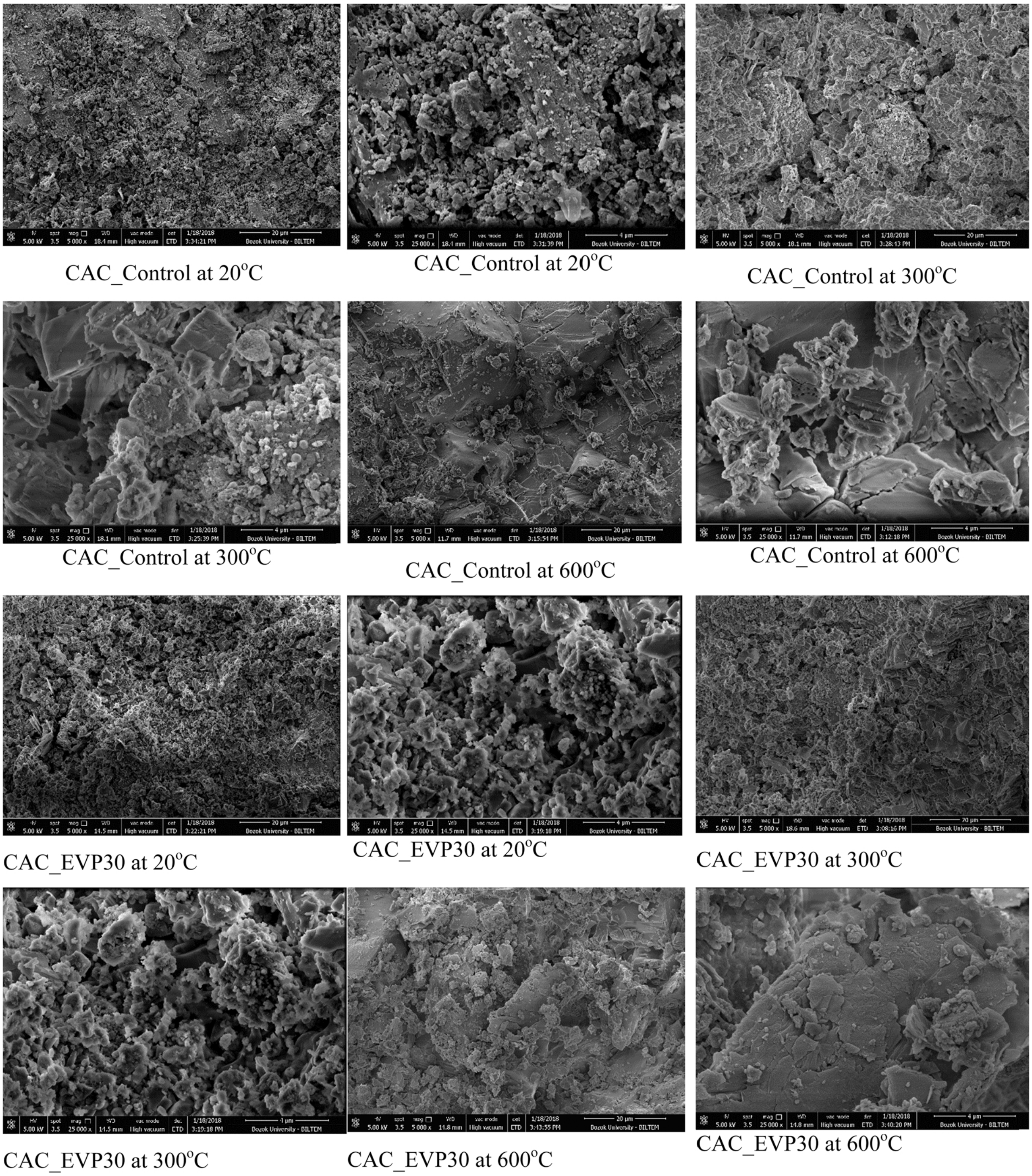

Fig. 19. SEM observations of CAC control and CAC EVP30 specimens after exposure to 20 °C, 300 °C and 600 °C.

- CAC specimens generally had lower thermal conductivity than PC specimens, but higher thermal conductivity reduction was obtained for PC specimens than CAC specimens at all temperature ranges.
- PC blended mortar had lower porosity, especially at 45% EVP replacement level than CAC blended mortar specimens at 600 °C temperature exposure.
- CAC blended mortar had a lower water absorption increase for CAC control and 15% and 30% EVP than PC blended mortar specimens at 300 °C temperature exposure. However, at 600 °C temperature exposure, CAC blended mortar had a higher water absorption increase than PC blended mortar specimens at all EVP rates.

Declaration of Competing Interest

The authors declare that they have no known competing financial interests or personal relationships that could have appeared to influence the work reported in this paper.

References

[1] G.A. Khoury, Compressive strength of concrete at high-temperatures - a reassessment, Mag. Concr. Res. 44 (161) (1992) 291–309.
[2] F. Arslan, A. Benli, M. Karatas, Effect of high temperature on the performance of self-compacting mortars produced with calcined kaolin and metakaolin, Constr. Build. Mater. 256 (2020), 119497.
[3] A. Benli, M. Karatas, H.A. Toprak, Mechanical characteristics of self-compacting mortars with raw and expanded vermiculite as partial cement replacement at elevated temperatures, Constr. Build. Mater. 239 (2020), 117895.
[4] M. Karatas, B. Balunb, A. Benli, High temperature resistance of self-compacting lightweight mortar incorporating expanded perlite and pumice, Comput. Concr. 19 (2) (2017) 121–126.
[5] M. Karatas, A. Benli, F. Arslan, The effects of kaolin and calcined kaolin on the durability and mechanical properties of self-compacting mortars subjected to high temperatures, Constr. Build. Mater. 265 (2020), 120300.
[6] M. Karatas, A. Benli, H.A. Toprak, Effect of incorporation of raw vermiculite as partial sand replacement on the properties of self-compacting mortars at elevated temperature, Constr. Build. Mater. 221 (2019) 163–176.
[7] S.M.A. El-Gamal, F.S. Hashem, M.S. Amin, Thermal resistance of hardened cement pastes containing vermiculite and expanded vermiculite, J. Therm. Anal. Calorim. 109 (1) (2012) 217–226.
[8] G.A. Khoury, Passive fire protection of concrete structures, Proc. Inst. Civil Eng Struct. B 161 (3) (2008) 135–145.
[9] G.T.G. Mohamedbhai, Effect of exposure time and rates of heating and cooling on residual strength of heated concrete, Mag. Concr. Res. 38 (136) (1986) 151–158.
[10] R. Sarshar, G.A. Khoury, Material and environmental-factors influencing the compressive strength of unsealed cement paste and concrete at high-Temperatures, Mag. Concr. Res. 45 (162) (1993) 51–61.
[11] F. Rostasy, R. Weiβ, G. Wiedemann, Changes of pore structure of cement mortars due to temperature, Cem. Concr. Res. 10 (2) (1980) 157–164.
[12] X. Zhang, G.X. Li, M.D. Niu, Z.P. Song, Effect of calcium aluminate cement on water resistance and high-temperature resistance of magnesium-potassium phosphate cement, Constr. Build. Mater. 175 (2018) 768–776.
[13] J.F. Zapata, M. Gomez, H.A. Colorado, Cracking in calcium aluminate cement pastes induced at different exposure temperatures, J. Mater. Eng. Perform. 28 (12) (2019) 7502–7513.
[14] J. Keriene, V. Antonovic, R. Stonys, R. Boris, The influence of the ageing of calcium aluminate cement on the properties of mortar, Constr. Build. Mater. 205 (2019) 387–397.
[15] M. Heikal, M.M. Radwan, O.K. Al-Duaij, Physico-mechanical characteristics and durability of calcium aluminate blended cement subject to different aggressive media, Constr. Build. Mater. 78 (2015) 379–385.
[16] W. Khaliq, H.A. Khan, High temperature material properties of calcium aluminate cement concrete, Constr. Build. Mater. 94 (2015) 475–487.
[17] C.H. Jiang, H.W. Yuan, C.H. Lu, Z.Z. Xu, D.Y. Lu, The effect of nanoparticles on the properties of calcium aluminate cement pastes at high temperatures, Adv. Cem. Res. 30 (5) (2018) 195–203.
[18] W. Fan, Y. Zhuge, X. Ma, C.W.K. Chow, N. Gorjian, J.A. Oh, W. Duan, Durability of fibre-reinforced calcium aluminate cement (CAC)-ground granulated blast furnace slag (GGBFS) blended mortar after sulfuric acid attack, Materials 13 (17) (2020).
[19] A. Abolhasani, H. Nazarpour, M. Dehestani, The fracture behavior and microstructure of calcium aluminate cement concrete with various water-cement ratios, Theor. Appl. Fract. Mech. 109 (2020), 102690.
[20] A. Terzic, J. Stojanovic, L. Andric, L. Milicic, Z. Radojevic, Performances of vermiculite and perlite based thermal insulation lightweight concretes, Sci. Sinter. 52 (2) (2020) 149–162.
[21] M. Roig-Flores, T. Lucio-Martin, M.C. Alonso, L. Guerreiro, Evolution of thermo-mechanical properties of concrete with calcium aluminate cement and special aggregates for energy storage, Cem. Concr. Res. 141 (2021), 106323.
[22] N.K. Lee, K.T. Koh, S.H. Park, G.S. Ryu, Microstructural investigation of calcium aluminate cement-based ultra-high performance concrete (UHPC) exposed to high temperatures, Cem. Concr. Res. 102 (2017) 109–118.
[23] A. Baradaran-Nasiri, M. Nematzadeh, The effect of elevated temperatures on the mechanical properties of concrete with fine recycled refractory brick aggregate and aluminate cement, Constr. Build. Mater. 147 (2017) 865–875.
[24] K.H. Mo, M.N. Hussin, T.-C. Ling, N.R. Sulong, F.W. Lee, C.W. Yuen, Development of lightweight aggregate mortar skin layer for an innovative sandwich concrete composite, J. Build. Eng. 27 (2020), 100941.
[25] K. Akçaözoğlu, S. Akçaözoğlu, The effect of elevated temperature on the lightweight concrete produced by expanded clay aggregate and calcium aluminate cement, Bilge Int. J. Sci. Technol. Res. 1 (2) (2017) 59–70.
[26] F. Koksal, O. Gencel, M. Kaya, Combined effect of silica fume and expanded vermiculite on properties of lightweight mortars at ambient and elevated temperatures, Constr. Build. Mater. 88 (2015) 175–187.
[27] F. Koksal, Y. Sahin, O. Gencel, Influence of expanded vermiculite powder and silica fume on properties of foam concretes, Constr. Build. Mater. 257 (2020), 119547.
[28] F. Koksal, M.A. Serrano-Lopez, M. Sahin, O. Gencel, C. Lopez-Colina, Combined effect of steel fibre and expanded vermiculite on properties of lightweight mortar at elevated temperatures, Mater. Struct. 48 (7) (2015) 2083–2092.
[29] M.M. Shoaib, S.A. Ahmed, M.M. Balaha, Effect of fire and cooling mode on the properties of slag mortars, Cem. Concr. Res. 31 (11) (2001) 1533–1538.
[30] R. Demirboga, R. Gul, The effects of expanded perlite aggregate, silica fume and fly ash on the thermal conductivity of lightweight concrete, Cem. Concr. Res. 33 (5) (2003) 723–727.
[31] R. Demirboga, R. Gul, Thermal conductivity and compressive strength of expanded perlite aggregate concrete with mineral admixtures, Energy Build. 35 (11) (2003) 1155–1159.
[32] S. Aydin, B. Baradan, Effect of pumice and fly ash incorporation on high temperature resistance of cement based mortars, Cem. Concr. Res. 37 (6) (2007) 988–995.

[33] H. Uysal, R. Demirboga, R. Sahin, R. Gul, The effects of different cement dosages, slumps, and pumice aggregate ratios on the thermal conductivity and density of concrete, Cem. Concr. Res. 34 (5) (2004) 845–848.
[34] O. Gencel, J.J. del Coz Diaz, M. Sutcu, F. Koksal, F.P. Alvarez Rabanal, G. Martinez-Barrera, W. Brostow, Properties of gypsum composites containing vermiculite and polypropylene fibers: numerical and experimental results, Energy Build. 70 (2014) 135–144.
[35] O. Gencel, F. Koksal, M. Sahin, M.Y. Durgun, H.E.H. Lobland, W. Brostow, Modeling of thermal conductivity of concrete with vermiculite by using artificial neural networks approaches, Exp. Heat Transf. 26 (4) (2013) 360–383.
[36] F. Koksal, J.J. del Coz Diaz, O. Gencel, F.P. Alvarez Rabanal, Experimental and numerical analysis of new bricks made up of polymer modified-cement using expanded vermiculite, Comput. Concr. 12 (3) (2013) 319–335.
[37] F. Koksal, O. Gencel, W. Brostow, H.E.H. Lobland, Effect of high temperature on mechanical and physical properties of lightweight cement based refractory including expanded vermiculite, Mater. Res. Innov. 16 (1) (2012) 7–13.
[38] F. Koksal, E. Mutluay, O. Gencel, Characteristics of isolation mortars produced with expanded vermiculite and waste expanded polystyrene, Constr. Build. Mater. 236 (2020), 117789.
[39] F. Koksala, J.J.D. Diaz, O. Gencel, F.P.A. Rabanal, Experimental and numerical analysis of new bricks made up of polymer modified-cement using expanded vermiculite, Comput. Concr. 12 (3) (2013) 319–335.
[40] ASTM, ASTM C1437 - 15 Standard Test Method for Flow of Hydraulic Cement Mortar, ASTM International, West Conshohocken, PA, 2015.
[41] ASTM C642 - 13 Standard Test Method for Density, Absorption, and Voids in Hardened Concrete, West Conshohocken, PA, ASTM International, 2013.
[42] ASTM, ASTM C348 - 19 Standard Test Method for Flexural Strength of Hydraulic-Cement Mortars, ASTM International, West Conshohocken, PA, 2019.
[43] ASTM, ASTM C349 - 18 Standard Test Method for Compressive Strength of Hydraulic-Cement Mortars (Using Portions of Prisms Broken in Flexure), ASTM International, West Conshohocken, PA, 2018.
[44] ASTM, ASTM C597-02, Standard Test Method for Pulse Velocity through Concrete, ASTM International, West Conshohocken, PA, 2003.
[45] ASTM D7984 - 16 Standard Test Method for Measurement of Thermal Effusivity of Fabrics Using a Modified Transient Plane Source (MTPS) Instrumen, ASTM International. 2016.
[46] P. Beroll, S. Schmalzl, D. Volkmer, Influence of surface-modification, length and volume fraction of carbon short fibers on the mechanical properties of calcium aluminate cement systems, Mater. Today Commun. 25 (2020), 101704.
[47] V. Pachta, S. Triantafyllaki, M. Stefanidou, Performance of lime-based mortars at elevated temperatures, Constr. Build. Mater. 189 (2018) 576–584.
[48] A.M. Rashad, Vermiculite as a construction material – a short guide for Civil Engineer, Constr. Build. Mater. 125 (2016) 53–62.
[49] S.M.A. El-Gamal, F.S. Hashem, M.S. Amin, Thermal resistance of hardened cement pastes containing vermiculite and expanded vermiculite, J. Therm. Anal. Calorim. 109 (1) (2011) 217–226.
[50] H. Binici, Y. Yardim, O. Aksogan, R. Resatoglu, A. Dincer, A. Karrpuz, Durability properties of concretes made with sand and cement size basalt, Sustain. Mater. Technol. 23 (2020), e00145.
[51] A.S.M.A. Awal, I.A. Shehu, M. Ismail, Effect of cooling regime on the residual performance of high-volume palm oil fuel ash concrete exposed to high temperatures, Constr.d Build. Mater. 98 (2015) 875–883.
[52] O. Gencel, A. Benli, O.Y. Bayraktar, G. Kaplan, M. Sutcu, W.A.T. Elabade, Effect of waste marble powder and rice husk ash on the microstructural, physico-mechanical and transport properties of foam concretes exposed to high temperatures and freeze–thaw cycles, Constr. Build. Mater. 291 (2021), 123374.
[53] O.Y. Bayraktar, G. Kaplan, O. Gencel, A. Benli, M. Sutcu, Physico-mechanical, durability and thermal properties of basalt fiber reinforced foamed concrete containing waste marble powder and slag, Constr. Build. Mater. 288 (2021), 123128.
[54] K.H. Mo, H.J. Lee, M.Y.J. Liu, T.-C. Ling, Incorporation of expanded vermiculite lightweight aggregate in cement mortar, Constr. Build. Mater. 179 (2018) 302–306.